JACS
JOURNAL OF THE AMERICAN CHEMICAL SOCIETY
Communication
pubs.acs.org/JACS

A New Polymer Nanoprobe Based on Chemiluminescence Resonance Energy Transfer for Ultrasensitive Imaging of Intrinsic Superoxide Anion in Mice

Ping Li, Lu Liu, Haibin Xiao, Wei Zhang, Lulin Wang, and Bo Tang*

College of Chemistry, Chemical Engineering and Materials Science, Collaborative Innovation Center of Functional-ized Probes for Chemical Imaging in Universities of Shandong, Key Laboratory of Molecular and Nano Probes, Ministry of Education, Shandong Provincial Key Laboratory of Clean Production of Fine Chemicals, Shandong Normal University, Jinan 250014, P. R. China

Supporting Information

ABSTRACT: Despite significant developments in optical imaging of superoxide anion ($O_2^{\bullet-}$) as the preliminary reactive oxygen species, novel visualizing strategies that offer ultrahigh sensitivity are still imperative. This is mainly because intrinsic concentrations of $O_2^{\bullet-}$ are extremely low in living systems. Herein, we present the rational design and construction of a new polymer nanoprobe PCLA-$O_2^{\bullet-}$ for detecting $O_2^{\bullet-}$ based on chemiluminescence (CL) resonance energy transfer without an external excitation source. Structurally, PCLA-$O_2^{\bullet-}$ contains two moieties linked covalently, namely imidazopyrazinone that is capable of CL triggered by $O_2^{\bullet-}$ as the energy donor and conjugated polymers with light-amplifying property as the energy acceptor. Experiment results demonstrate that PCLA-$O_2^{\bullet-}$ exhibits ultrahigh sensitivity at the picomole level, dramatically prolonged luminescence time, specificity, and excellent biocompatibility. Without exogenous stimulation, this probe for the first time in situ visualizes $O_2^{\bullet-}$ level differences between normal and tumor tissues of mice. These exceptional features ensure that PCLA-$O_2^{\bullet-}$ as a self-luminescing probe is an alternative in vivo imaging approach for ultralow level $O_2^{\bullet-}$.

Reactive oxygen species (ROS) produced in living systems are usually tamed as cellular redox balances maintained by enzymatic and nonenzymatic antioxidant defenses.[1] Although ROS contribute to cellular functions, any disruption of their physiologic homeostasis could potentially lead to serious issues,[2,3] such as cancer, diabetes, neurodegeneration, and other disorders. Noteworthily, the superoxide radical ($O_2^{\bullet-}$) is one of the primary ROS[4] and acts as a sink for many other radicals generated intracellularly. Consequently, the highly sensitive and specific detection of $O_2^{\bullet-}$ in biological systems has received growing attention. In particular, noninvasive in vivo fluorescent imaging associated with easy operation molecule probes and nanoprobes becomes an attractive avenue for elucidating its biological function. However, because of very low actual concentration in biological systems, the detection of endogenous $O_2^{\bullet-}$ in tissues and in vivo employing molecular probes or nanoprobes without stimulation has not been realized so far.

Chemiluminescence (CL) with imidazopyrazinone[5−7] is a well-established technology applied to biological analysis of $O_2^{\bullet-}$. This is attributed to no external light excitation, offering many prominent advantages over traditional photon emission-based detection methods, such as significantly reduced background fluorescence interference and photodamage, and so on. Despite these appealing features, there remains substantial stumbling blocks to the routine use of CL as an optical imaging strategy for $O_2^{\bullet-}$, for instance, low emission intensity, short CL time, and short emission wavelength. To solve the above problems, chemiluminescence resonance energy transfer (CRET) provides good opportunities,[8−10] because CRET can effectively prolong luminescence time and cause wavelength red-shift. In the meantime, conjugated polymers (CPs)[11−15] as fluorophores are endowed with high absorptivity, extraordinary brightness, and excellent biocompatibility as well as easy fabrication. Their fascinating properties bring out booming developments in imaging probes. Based on distinguished signal amplification along the backbone and adjustable optical performance, CPs are suitable candidates as the energy receptors of CRET process. Importantly, a hydrophobic environment of CPs nanoparticle interior can further boost CL intensity and extend luminescence time.[5,8] Moreover, unlike fluorescence resonance energy transfer (FRET), CRET,[16,17] the nonradiative resonance energy-transfer process, we suppose that a higher efficiency can be achieved through covalent link between the acceptor and the donor than physical integration. Furthermore, previous studies suggest that covalent attachments not only provide a readily energy transfer but also avoid the leakage problem of small molecules encapsulated in nanoparticles.[18] Therefore, in order to highly sensitive imaging intrinsic $O_2^{\bullet-}$ of ultralow concentration in vivo, development of the conjugated polymer probe based on CRET by covalent attachment is of great value.

Here, we report an in vivo imaging platform for native $O_2^{\bullet-}$ based on CRET. As illustrated in the Scheme 1, the designed probe termed PCLA-$O_2^{\bullet-}$ comprises two segments connected through the covalent bond. Structurally, imidazopyrazinone moiety (CLA for short) acts as both recognition unit of $O_2^{\bullet-}$ and the energy donor, while CPs (PFBT)[19] with quaternary ammonium groups act as both the energy acceptor and signal amplification matrix.[13] Using nanoprecipitation,[12] PCLA-$O_2^{\bullet-}$ polymer chains covalently attaching the multiple antennas

Received: November 13, 2015
Published: February 24, 2016

DOI: 10.1021/jacs.5b11784
J. Am. Chem. Soc. 2016, 138, 2893−2896

Scheme 1. Schematic Illustration of Nanoparticles Preparation by "Nanoprecipitation" and $O_2^{\bullet-}$ Sensing of PCLA-$O_2^{\bullet-}$ and the Structure of PCLA-$O_2^{\bullet-}$

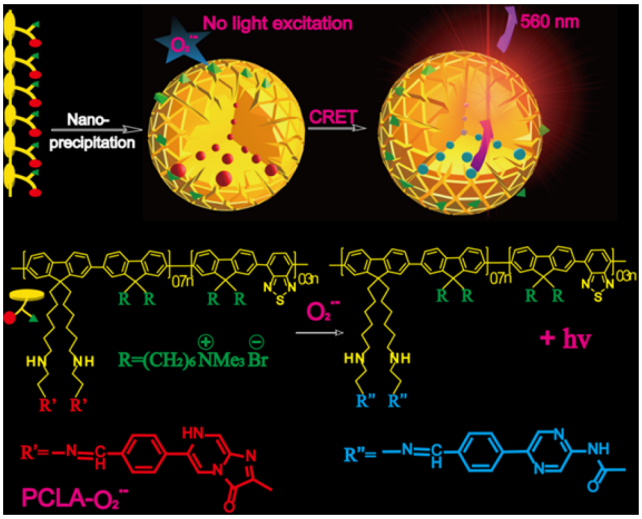

(CLA) fold to form compact spherical nanoparticles in aqueous medium. As a result, the nanoparticles can afford a hydrophobic interior, in which CLA parts are embedded. Once the $O_2^{\bullet-}$ is added, through a radiationless energy-transfer process, the energy produced by specific reaction between CLA and $O_2^{\bullet-}$ is transferred to PFBT with nonemitting of green light (λ_{max}, 490 nm). Afterward, the PFBT acceptor can be excited and emits magnified light (λ_{max}, 560 nm). Based on the above principle, the novel nanoprobe was fabricated. As expected, this CRET system enables successful live imaging of $O_2^{\bullet-}$ in mice.

PCLA-$O_2^{\bullet-}$ was synthesized from PFBT with quaternary ammonium groups and CHO-CLA with imidazopyrazinone (Schemes S1 and S2). The specific synthetic routes and characterization of PFBT, CHO-CLA, and PCLA-$O_2^{\bullet-}$ are shown in the Supporting Information. FT-IR spectroscopy in Figure S1 showed that 1723 cm^{-1} strong peak is assigned to C═N bond, indicating the covalent conjugation of CLA to PFBT. Finally, nanoparticles of PCLA-$O_2^{\bullet-}$ were prepared by nanoprecipitation, after addition of PCLA-$O_2^{\bullet-}$ solution in tetrahydrofuran (THF) into excessive water. The physical properties of this nanoprobe were investigated by the high-resolution transmission electronmicroscopy (HRTEM) and dynamic light scattering (DLS). As is clearly visible from the HRTEM images (Figure 1a), spherical morphology of nanoparticles was confirmed. Their average diameters were about 20 nm, consistent with the results obtained in DLS experiments (Figure 1b). Moreover, potentiometric analysis displayed that $Z_{potential}$ was +49 mV, which should be owing to hydrophilic quaternary ammonium groups on the surface of the nanoparticles. Together, these data manifest that PCLA-$O_2^{\bullet-}$ nanoprobe has been constructed successfully in full accordance with the design.

Subsequently, we compared the optical properties of PCLA-$O_2^{\bullet-}$, PFBT, and CHO-CLA. Figure 1c showed that the absorption peaks of PFBT were at 350 and 470 nm, meanwhile the CL peak of CHO-CLA centered at 490 nm in the presence of $O_2^{\bullet-}$. Obviously, there was overlap between absorption spectrum of the PFBT and luminescence spectrum of CHO-CLA, meaning distinct possibility of CRET occurrence. Next, whether $O_2^{\bullet-}$ can make PCLA-$O_2^{\bullet-}$ self-emitting by CRET was examined. Upon addition of $O_2^{\bullet-}$, without any external light excitation, intense

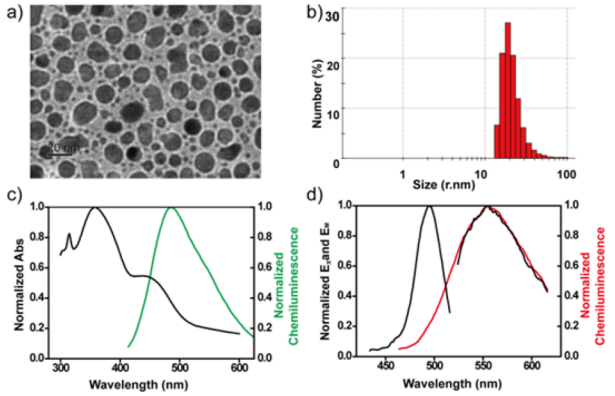

Figure 1. (a) HRTEM image of PCLA-$O_2^{\bullet-}$ in water. Scale bar = 20 nm. (b) DLS image of PCLA-$O_2^{\bullet-}$. (c) Absorption spectrum of PFBT (black line) and CL spectrum of CHO-CLA (green line). (d) Excitation/emission spectra (black lines) and CL spectrum (red line) of PCLA-$O_2^{\bullet-}$ in PBS (10 mM, pH = 7.4). CL is detected in the presence of 10 μM $O_2^{\bullet-}$.

luminescence was observed at 560 nm of longer wavelength (Figure 1d), confirming efficient CRET in PCLA-$O_2^{\bullet-}$ from CLA to PFBT. To further verify the validity of CRET, a control experiment was performed in a mixed aqueous solution of CHO-CLA and PFBT. As illustrated in Figure S2, CL intensities of PFBT in the control experiment remained almost unchanged under the same condition, even with increasing amount of CHO-CLA. This may be because a part of CHO-CLA dispersed in the mixed solvent. Therefore, these results not only demonstrate the successful covalent conjugation of CLA to PFBT but also highlight its necessary covalent linkage by controlling close distance between CLA and PFBT, resulting in an efficient CRET.

Then, the CL responses of PCLA-$O_2^{\bullet-}$ toward different concentrations of $O_2^{\bullet-}$ were examined in PBS buffer (pH 7.4). Figure 2 revealed, when $O_2^{\bullet-}$ level was elevated, the CL signals were pronouncedly intensified. The output of images showed CL intensities increased linearly with the concentrations of $O_2^{\bullet-}$ in the range from 0 to 950 pM (Figure 2). The detection limit was estimated to be 19.3 pM, as calculated by equation LOD = $3S_0/K$. To the best our knowledge, up to now, this is the most sensitive luminescence probe for $O_2^{\bullet-}$ compared with nanomolar level of

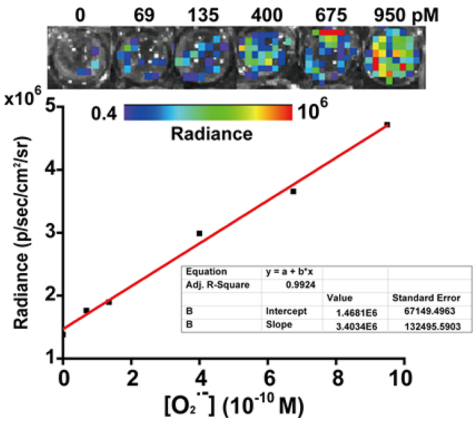

Figure 2. Linear relationship between CL of PCLA-$O_2^{\bullet-}$ and [$O_2^{\bullet-}$] (0–950 pM) (PCLA-$O_2^{\bullet-}$ = 0.45 mg/mL, PBS = 10 mM, pH = 7.4, 10% THF). Inset, CL images of PCLA-$O_2^{\bullet-}$ in response to indicated concentrations of $O_2^{\bullet-}$ by an IVIS Lumina II in vivo imaging system with open filter (570 ± 10 nm).

DOI: 10.1021/jacs.5b11784
J. Am. Chem. Soc. 2016, 138, 2893–2896

reported probes. Furthermore, upon addition of various other reactive species (H_2O_2, $^1O_2$, NO, ascorbic acid, ClO^-, TBHP, •OH, GSH, $ONOO^-$), there were negligible CL responses of PCLA-$O_2^{\bullet-}$ (Figure S3). And also, the CL of PCLA-$O_2^{\bullet-}$ in response to $O_2^{\bullet-}$ was independent of pH in the physiological range (Figure S4) and serum (Figure S5). Meanwhile, Figure S6 reflects the excellent stability of PCLA-$O_2^{\bullet-}$ without $O_2^{\bullet-}$ over time. Thus, PCLA-$O_2^{\bullet-}$ turns out to be extremely sensitive and selective to $O_2^{\bullet-}$.

To test whether our design strategy gives rise to more luminescent time, delayed luminescence (DL) of CHO-CLA and PCLA-$O_2^{\bullet-}$ were investigated, respectively. After addition of $O_2^{\bullet-}$, the CL channels of the PCLA-$O_2^{\bullet-}$ (λ_{em} = 570 ± 10 nm) and CHO-CLA (λ_{em} = 520 ± 10 nm) were imaged over time, depicted as in Figure 3. It is can be seen that the CL intensities of

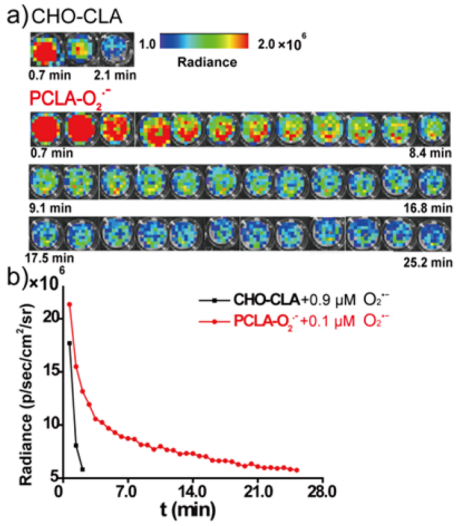

Figure 3. (a) CL images of CHO-CLA (λ_{em} = 520 ± 10 nm) and PCLA-$O_2^{\bullet-}$ (λ_{em} = 570 ± 10 nm) in response to $O_2^{\bullet-}$ (0.9 and 0.1 μM, respectively) over time (CHO-CLA = 4.2 mM, PCLA-$O_2^{\bullet-}$ = 0.45 mg/mL, PBS = 10 mM, pH = 7.4, 10% THF). (b) Quantitative CL intensities of CHO-CLA and PCLA-$O_2^{\bullet-}$ as a function of time.

CHO-CLA attenuated dramatically in 2.1 min (Figure 3b). However, luminescence of PCLA-$O_2^{\bullet-}$ obviously lasted much longer. The results suggest that a hydrophobic environment of CPs nanoparticle interior and effective CRET by covalent link[5,18] indeed lengthen the duration of DL for $O_2^{\bullet-}$. This fascinating merit is crucial and favorable for a practical application of biological imaging.

All these optical and photophysical advantages of PCLA-$O_2^{\bullet-}$ make it a promising nanoplatform for in vivo $O_2^{\bullet-}$ imaging. With the PCLA-$O_2^{\bullet-}$ in hand, we started to validate its biological feasibility for detecting $O_2^{\bullet-}$. First, we texted $O_2^{\bullet-}$ levels in macrophages extracts utilizing PCLA-$O_2^{\bullet-}$, phorbol 12-myristate 13-acetate (PMA)[20] as activator to elevate $O_2^{\bullet-}$ levels. The CL (λ_{em} = 570 ± 10 nm) response imaging (pseudocolor) of PCLA-$O_2^{\bullet-}$ toward $O_2^{\bullet-}$ was carried out under four different conditions. The experiment results summarized in Figure S7a showed that PCLA-$O_2^{\bullet-}$ strongly emitted CL in extracts from PMA-stimulated macrophages. The CL intensity increased by 3.6×, as a comparison with the control without PMA treatment. At the same time, superoxide dismutases (SOD) and Tiron,[21] the free-radical ($O_2^{\bullet-}$) scavengers, were used to treat macrophages pre-incubated with PMA respectively. We found that CL signals were markedly suppressed, indicating the successful scavenging of $O_2^{\bullet-}$. Furthermore, PCLA-$O_2^{\bullet-}$ was used to monitor intrinsic $O_2^{\bullet-}$ in a nonmetastatic human mammary epithelial cell line (MCF-10A) and mouse mammary carcinoma cells (4T1), respectively. As shown in Figure S7b, CL intensity in the 4T1 extracts was 2.1× higher than that of MCF-10A extracts, reflecting higher level $O_2^{\bullet-}$ in tumor cells. These in vitro data clearly substantiate that PCLA-$O_2^{\bullet-}$ has the capability of specifically sensing native $O_2^{\bullet-}$ in biological samples and also differentiating normal cells and tumor cells by variant $O_2^{\bullet-}$ levels. Additionally, PCLA-$O_2^{\bullet-}$ was found to be nontoxic to cells and mice (Figure S8).

Based on the above-discussed results, PCLA-$O_2^{\bullet-}$ possesses the distinguished advantages over the existing small molecule CL compounds, we consider that PCLA-$O_2^{\bullet-}$ may in situ detect the fluctuations of $O_2^{\bullet-}$ in vivo. As reported, excessively produced $O_2^{\bullet-}$ is implicated in the development of numerous inflammatory diseases.[22] Thereby, PCLA-$O_2^{\bullet-}$ was used to evaluate the endogenous $O_2^{\bullet-}$ in mice with inflammation without an external excitation, which can remarkably improve sensitivity and reduce photodamage. Different groups of mice were treated with intraperitoneally (i.p.) administrated lipopolysaccharide (LPS)[23] for inducing acute inflammation (I), LPS + Tiron(II), saline and PCLA-$O_2^{\bullet-}$ (III), and saline (IV), respectively. Then, CL (λ_{em} = 570 ± 10 nm) images were acquired. We found PCLA-$O_2^{\bullet-}$ displayed much brighter CL in LPS-treated mice than that of only PCLA-$O_2^{\bullet-}$-treated (Figure 4a). Notably, CL intensity in

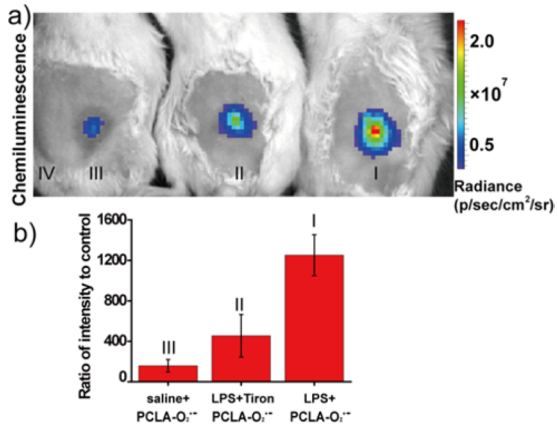

Figure 4. (a) The CL imaging of endogenous $O_2^{\bullet-}$ in the LPS-treated mice (n = 4). (I) LPS was injected into peritoneal cavity of mice, after 4 h, followed by injection PCLA-$O_2^{\bullet-}$ (0.068 mg). (II) LPS was injected into abdomen, after 3 h, followed by injection Tiron (400 μL, 10 μM). PCLA-$O_2^{\bullet-}$ (0.068 mg) was injected 1 h later. (III) Saline + PCLA-$O_2^{\bullet-}$ (0.068 mg). (IV) The control: saline. (b) Quantitative of CL emission intensities from groups (I–IV) at 0.5 min.

the LPS-treated group was 7.9× higher than that of the only PCLA-$O_2^{\bullet-}$-treated group (Figure 4b), meaning a rise of [$O_2^{\bullet-}$]. In contrast, upon the injection of Tiron to the LPS-pretreated mouse, CL intensity weakened distinctly. Meanwhile, Figure 4a IV demonstrated that there was no emission in the group with only saline injection, indicating no background fluorescence. Apparently, owing to no interference from biological autofluorescence, effective CRET, and interior hydrophobic conditions of this nanoprobe, imaging quality and sensitivity were significantly upgraded. Moreover, Figure S9 demonstrates that enough long luminescence time was beneficial to conveniently monitor $O_2^{\bullet-}$. Altogether, we conclude that

DOI: 10.1021/jacs.5b11784
J. Am. Chem. Soc. 2016, 138, 2893–2896

PCLA-$O_2^{\bullet-}$ allows for in situ imaging of the $O_2^{\bullet-}$ in vivo by means of CL.

To further assess the practicability of PCLA-$O_2^{\bullet-}$ to spy on intrinsic $O_2^{\bullet-}$ in the absence of stimulation, we examined whether it could distinguish the difference in $O_2^{\bullet-}$ concentrations between normal and tumor tissues in mice. A mouse mammary carcinoma model was constructed by injecting 4T1 cells in forelimb armpit. After 10 days, a tumor mass was obtained. Then, PCLA-$O_2^{\bullet-}$ (0.068 mg) was injected in tumor (I), tumor + Tiron(II), and normal (III) tissues of the mice, respectively. Subsequently, we found PCLA-$O_2^{\bullet-}$ displayed much stronger CL in tumor tissue than that of normal tissue (Figure 5a). The CL intensity was 3.0× higher than the normal

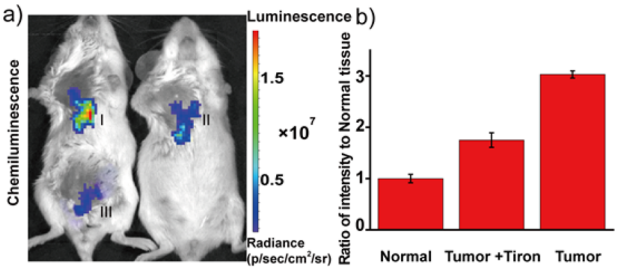

Figure 5. a) Representative images (pseudocolor) of mice in vivo tumor (I), tumor + Tiron(II) and normal (III) tissues followed by PCLA-$O_2^{\bullet-}$ (n = 3). Images (λ_{em} = 570 ± 10 nm) were acquired using an IVIS Lumina II at 30 s after PCLA-$O_2^{\bullet-}$ administration. (b) Quantitative CL intensities of (I–III).

tissue (Figure 5b), indicating noticeably higher levels of $O_2^{\bullet-}$ in the tumor tissue. Meanwhile, weak CL signal in tumor tissue was observed after injection of Tiron. The results presented here validate for the first time visualization of the $O_2^{\bullet-}$ native variance without stimulation in small animals.

In summary, we describe a supersensitive imaging nanoprobe PCLA-$O_2^{\bullet-}$ for $O_2^{\bullet-}$ based on CRET between imidazopyrazinone and conjugated polymers. Without an external excitation source, the attractive probe was applied in mice to selectively visualize $O_2^{\bullet-}$ in normal/inflammation tissues. More importantly, as the most sensitive $O_2^{\bullet-}$ probe to our knowledge, PCLA-$O_2^{\bullet-}$ revealed native concentration differences of $O_2^{\bullet-}$ between normal and tumor tissues without exogenous stimulation. The above breakthroughs achieved are attributed to several remarkable advantages of the new imaging probe: (1) elevated CRET efficiency by a covalent link between acceptor and donor, (2) substantially extended luminescence time due to effective CRET process, (3) significantly enhanced CL intensity under interior hydrophobic environment via polymer nanoparticle formation, (4) greatly improved sensitivity and imaging resolution owing to longer luminescence time and no background fluorescence interference without external light source. We deem that PCLA-$O_2^{\bullet-}$ would serve as a powerful tool to differentiate normal and pathological tissues via distinguishing $O_2^{\bullet-}$ concentrations. These interesting results and limited tissue penetration capability of 560 nm prompt us to develop the new near-infrared probe for deep tissue imaging and clinical applications in superoxide anion related biological and medical research. And also, we can investigate the similar CRET platforms to visualize other active molecules in vivo.

■ ASSOCIATED CONTENT

Supporting Information

The Supporting Information is available free of charge on the ACS Publications website at DOI: 10.1021/jacs.5b11784.

Experimental details and data (PDF)

■ AUTHOR INFORMATION

Corresponding Author

*tangb@sdnu.edu.cn

Notes

The authors declare no competing financial interest.

■ ACKNOWLEDGMENTS

This work was supported by 973 Program (2013CB933800) and National Natural Science Foundation of China (21390411, 21535004, 21227005, 21475079, and 21305080).

■ REFERENCES

(1) Fruehauf, J.; Meyskens, F. *Clin. Cancer Res.* **2007**, *13*, 789–794.
(2) Dröge, W. *Physiol. Rev.* **2002**, *82*, 47–95.
(3) Gorrini, C.; Harris, I. S.; Mak, T. W. *Nat. Rev. Drug Discovery* **2013**, *12*, 931–947.
(4) Dickinson, B. C.; Chang, C. J. *Nat. Chem. Biol.* **2011**, *7*, 504–511.
(5) Teranishi, K. *Bioorg. Chem.* **2007**, *35*, 82–111.
(6) Sekiya, M.; Umezawa, K.; Sato, A.; Citterio, D.; Suzuki, K. *Chem. Commun.* **2009**, 3047–3049.
(7) Teranishi, K.; Nishiguchi, T. *Anal. Biochem.* **2004**, *325*, 185–195.
(8) Shuhendler, A. J.; Pu, K.; Cui, L.; Uetrecht, J. P.; Rao, J. H. *Nat. Biotechnol.* **2014**, *32*, 373–380.
(9) Xiong, L. Q.; Shuhendler, A. J.; Rao, J. H. *Nat. Commun.* **2012**, *3*, 1193–1200.
(10) Roda, A.; Guardigli, M. *Anal. Bioanal. Chem.* **2012**, *402*, 69–76.
(11) Li, K.; Liu, B. *Chem. Soc. Rev.* **2014**, *43*, 6570–6597.
(12) Feng, L.; Zhu, C.; Yuan, H.; Liu, L.; Lv, F.; Wang, S. *Chem. Soc. Rev.* **2013**, *42*, 6620–6633.
(13) Swager, T. M. *Acc. Chem. Res.* **1998**, *31*, 201–207.
(14) Liu, J.; Lam, J. W. Y.; Tang, B. Z. *Chem. Rev.* **2009**, *109*, 5799–5867.
(15) Wu, C.; Chiu, D. T. *Angew. Chem., Int. Ed.* **2013**, *52*, 3086–3109.
(16) Freeman, R.; Liu, X.; Willner, I. *J. Am. Chem. Soc.* **2011**, *133*, 11597–11604.
(17) Liu, X.; Freeman, R.; Golub, E.; Willner, I. *ACS Nano* **2011**, *5*, 7648–7655.
(18) Wu, I. C.; Yu, J.; Ye, F.; Rong, Y.; Gallina, M. E.; Fujimoto, B. S.; Zhang, Y.; Chan, Y. H.; Sun, W.; Zhou, X. H.; Wu, C.; Chiu, D. T. *J. Am. Chem. Soc.* **2015**, *137*, 173–178.
(19) Liu, B.; Bazan, G. C. *Nat. Protoc.* **2006**, *1*, 1698–1702.
(20) Maeda, H.; Yamamoto, K.; Nomura, Y.; Kohno, I.; Hafsi, L.; Ueda, N.; Yoshida, S.; Fukuda, M.; Fukuyasu, Y.; Yamauchi, Y.; Itoh, N. *J. Am. Chem. Soc.* **2005**, *127*, 68–69.
(21) Zorov, D. B.; Filburn, C. R.; Klotz, L. O.; Zweier, J. L.; Sollott, S. J. *J. Exp. Med.* **2000**, *192*, 1001–1014.
(22) Afonso, V.; Champy, R.; Mitrovic, D.; Collin, P.; Lomri, A. *Jt., Bone, Spine* **2007**, *74*, 324–329.
(23) Lee, D.; Khaja, S.; Velasquez-Castano, J. C.; Dasari, M.; Sun, C.; Petros, J.; Taylor, W. R.; Murthy, N. *Nat. Mater.* **2007**, *6*, 765–769.

DOI: 10.1021/jacs.5b11784
J. Am. Chem. Soc. 2016, 138, 2893–2896